Steel and Composite Structures, *Vol. 31, No. 2 (2019) 159-172*
DOI: https://doi.org/10.12989/scs.2019.31.2.159

Parametric study of shear strength of CFRP strengthened end-web panels

Haitham A. Shalaby [1a], Maha M. Hassan [*1,2] and Sherif S. Safar [1b]

[1] *Structural Engineering Department, Cairo University, Gamaet El Qahera Street, Egypt*
[2] *Civil Engineering Department, University of Prince Mugrin, Medina, Saudi Arabia (On leave from Cairo University)*

(*Received May 2, 2018, Revised March 20, 2019, Accepted March 31, 2019*)

Abstract. Strengthening of civil infrastructure with advanced composites have recently become one of the most popular methods. The use of Fiber Reinforced Polymer (FRP) strips plates and fabric for strengthening of reinforced concrete structures has well established design guidelines and standards. Research on the application of FRP composites to steel structures compared to concrete structures is limited, especially for shear strengthening applications. Whereas, there is a need for cost-effective system that could be used to strengthen steel high-way bridge girders to cope with losses due to corrosion in addition to continuous demands for increasing traffic loads. In this study, a parametric finite element study is performed to investigate the effect of applying thick CFRP strips diagonally on webs of plate girders on the shear strength of end-web panels. The study focuses on illustrating the effect of several geometric parameters on nominal shear strength. Hence, a formula is developed to determine the enhancement of shear strength gained upon the application of CFRP strips.

Keywords: finite element; Carbon Fiber Reinforced Polymer (CFRP); plate girders; strengthening

1. Introduction

FRP materials have offered great potential in the repair and rehabilitation of different structural members. They hold numerous benefits over traditional repair methods. FRP materials are characterized by high strength-to-weight ratio, corrosion resistance in addition to easy application through bonding. Numerous economic effects are gained due to low transportation and handling costs as well as low application and labor costs. Moreover, FRP is less disruptive to regular service during the repair process. Furthermore, repairs that employ FRP contribute the minimum additional dead load to the structure. Bonded FRP strengthening also creates less stress concentration to the repaired structural elements as compared to repair techniques including mechanical or welding fastening.

In the last decades, a significant amount of research has established the successful use of CFRP materials for strengthening of concrete structures. With the introduction of ultra-high modulus CFRP materials, the probability of forming a successful strengthening method for steel structures using FRP materials has emerged due to their relatively higher tensile strength and stiffness. In addition, high demand on strengthening steel structures which were built during the last two centuries is a pressing issue. The application of FRP materials to steel structures is widely established for flexure and shear strengthening where the uni-directional strength of FRP materials can significantly be utilized. Use of CFRP strips to repair critical areas of tension flanges of steel members, composite steel-concrete girders and unstiffened steel I-section beams was tested by many researchers (Park and Yoo 2015, Wang *et al*. 2017 and Elchalakani and Fernando 2012). Authors reported significant improvement of values of ultimate loads. Ardalani *et al*. (2017) reported that using CFRP plates to strengthen plate girders subjected to three point bending enhances the stiffness and resistance in addition to changing failure mechanism of the plate girders.

Miller *et al*. (2001) reviewed research efforts performed regarding the use of CFRP in strengthening of steel bridge girders. Rizkalla *et al*. (2017) explored the research efforts performed to employ small diameter CFRP strands for shear strengthening of steel structures and bridges and design guidelines were proposed accordingly. Bocciarelli *et al*. (2018) performed experimental and parametric analyses in order to investigate the effectiveness of using CFRP plates on fatigue crack propagation of notched steel beams.

Narmashiri *et al*. (2010) studied the effect of shear strengthening of stiffened steel I-beams using CFRP plates through testing of five steel beams under two-point bending. The different beams had identical geometric properties with different strengthening schemes: Two or three strips of CFRP plates were placed on single side or both sides of webs covering the shear zone area. Authors found that loading capacities increased by ratios ranging between 30-50% depending on the strengthening scheme. Okuyama *et al*. (2012) tested strengthened steel beams while considering a wider range of geometric properties including aspect ratio of web, type of CFRP strips, and fiber orientation angles. CFRP strips were oriented diagonally in both the tension and compression field directions. Enhancements to the maximum attained loading capacity were reported depending upon the orientation angle of

*Corresponding author, Associate Professor,
E-mail: mahamoddather@eng.cu.edu.eg
[a] Graduate Student
[b] Professor

ISSN: 1229-9367 (Print), 1598-6233 (Online)

added strips. May and Bhutto (2013) experimentally investigated the enhancement of the shear strength of stiffened steel I-beam considering two strengthening methods. The first method included using GFRP in the shape of T-sections as additional stiffener placed on one side or both sides of the web at different locations of the beam. The second method included strengthening using four or eight layers of GFRP or four layers of CFRP to one side of the end-web panels. Reported enhancements ranged between 20–54% of the maximum peak load for un-strengthened beams. Safar and Abou-Zeid (2014) tested twelve stiffened steel I-beams strengthened with CFRP strips applied on the diagonal principal stresses direction on elastic end-web panel. One or three CFRP strips were bonded on single side or both sides of webs. The studied parameters included web aspect ratio, slenderness ratio of web, flange width-to-thickness ratio. Test results showed that applying intermediate modulus CFRP strips on the web did not enhance the buckling load as all webs were proportioned to buckle in the elastic range. Meanwhile, the value of the ultimate shear strength increased by percentages ranging between 6–120% for the different strengthened steel beams. The observed improvements were attributed to the increase of post-buckling strength resulting from additional tension forces supported by the CFRP strips and reduction of tensile strains in the web after buckling.

The current study is an extension of the experimental study performed by Safar and Abou-Zeid (2014). Finite element models are built and verified against the experimental results. Hence, an extensive parametric study is initiated and the effect of different key parameters is considered. Accordingly, a mathematical model is developed to determine the enhancement in shear strength after adding CFRP strips in the diagonal direction of plate girder webs.

2. Shear strength of end-web panels

Webs in plate girders are essentially used to maintain a reasonable distance between the two flange plates. Flanges mainly resist the applied moment, whereby the web resists shear forces. In plate-girders, shear buckling of thin web panels takes place when the applied shear exceeds the critical shear stress of the web panel. After buckling, diagonal tensile membrane stress field carry any additional load. Failure takes place when the web yields across the tensile stress field and plastic hinges develop in the top and bottom flanges. Due to the large slenderness ratio of plate girder webs, shear buckling is usually achieved at an early stage of loading. In order to increase their buckling strength, webs are commonly strengthened with transversal or longitudinal stiffeners.

Wagner (1931) noted the post buckling strength of web panels and pointed out the uniform diagonal tension field developing in web plates after buckling. Basler (1961) developed a theory estimating the shear strength of slender web plates. Basler assumed that the diagonal tension field fully yielded and that the vertical component of the diagonal tension was equilibrated by axial compressive force supported by transverse stiffener. Hence, diagonal tension field cannot develop in the web without the existence of appropriate anchoring mechanism in flanges and adjacent web panels. Accordingly, Basler theory does not consider the effect of post buckling shear strength of end-web panels, V_{pb}, due to interruption of the continuity of equilibrium. For intermediate web panels, the nominal shear strength, V_n, was calculated by summing the elastic buckling load, V_{cr}, and post-buckling load, V_{pb}. Timoshenko and Gere (1961) established a theoretical closed form solution for V_{cr} as follows

$$V_{cr} = h.t_w.k.\frac{\pi^2 E}{12(1-\mu^2)(h/t_w)^2} \tag{1}$$

Where h is depth of the web plate, t_w is thickness of web plate, E is Young's modulus, and k is the buckling coefficient which depends on the aspect ratio (a/h) and boundary conditions of web plate.

Meanwhile, for intermediate web panel only, the post buckling load can be calculated as follows

$$V_{pb} = \frac{V_y - V_{cr}}{1.15\sqrt{1+(a/h)^2}} \tag{2}$$

Due to the conservatism of Basler's theory with respect to end-web panels, Hoglund (1972) developed formulas estimating the shear strength of end-web panels. For webs in pure shear, the elastic buckling occurs at a significant less value than the nominal shear strength. Therefore, the anchoring system presented in the surrounding flanges and transverse stiffeners provide a substantial post-buckling strength after buckling. The inclination of tensile principle stresses is defined by an angle (Φ) which is affected by the value of V_u/V_{cr}. Accordingly, the shear buckling load is estimated as

$$V_w = \rho_v.f_{yw}.h.t_w \tag{3}$$

Where h is the height of web plate, t_w is thickness of the web plate, f_{yw} is the yielding stress of the web and ρ_v is the shear buckling reduction factor as defined in Table 1.

Safar (2013) established a mathematical model for the shear strength of end-web panels of steel plate girders considering the case including non-rigid end post based on a comprehensive numerical investigation. The study included analyzing sixty-four finite element models using ANSYS software program. Results showed that end-web panels possessed post-buckling strength where diagonal

Table 1 Reduction factor ρ_v

λ_w	Rigid End Post (Steel)	Non-Rigid End Post (Steel)
$\lambda_w < 0.48/\eta$	η	η
$0.48/\eta \le \lambda_w < 1.08$	$\frac{0.48}{\lambda_w}$	$\frac{0.48}{\lambda_w}$
$\lambda_w \ge 1.08$	$\frac{0.79}{(0.7+\lambda_w)}$	$\frac{0.48}{\lambda_w}$

tension stresses were equilibrated by compressive stresses in end-bearing stiffeners and portions of the web stiffened by flanges and stiffeners. It was found that flanges will only enhance the boundary conditions of the web-panel and buckling coefficient (k). Hence, boundary condition of the web at flanges are closer to fixation than simple supports. Accordingly, expressions were proposed for estimating the nominal shear strength of end-web panels while including the tension-field action as follows

For web yielding: $\lambda \leq 1.112$

$$V_n = V_y \tag{4}$$

For inelastic web buckling: $1.112 \leq \lambda \leq 1.39$

$$V_n = \frac{1.112}{\lambda}.V_y \tag{5}$$

For elastic web buckling: $\lambda \geq 1.39$

$$V_n = V_y.\left[\frac{1.546}{\lambda^2} + \frac{0.6}{(a/h)+12}(1-\frac{1.546}{\lambda^2}).\sqrt[6]{\frac{E.k}{f_y}(\lambda^2 - 1.932)}\right] \tag{6}$$

Where

$$v_y = 0.58.f_y.h.t_w \tag{7}$$

$$\lambda = \frac{h}{t_w} \cdot \sqrt{\frac{f_y}{E.k}} \tag{8}$$

$$k = k_{ss} + (0.0009t_f/t_w + 0.3)(k_{sf} - k_{ss}) \leq k_{sf} \tag{9}$$

For $a/h \geq 1.0$:

$$k_{ss} = 2.34 + \frac{4.0}{(a/h)^2} \tag{10}$$

For $a/h \geq 1.0$:

$$k_{sf} = \frac{4.0}{(a/h)^2} - \frac{1.99}{(a/h)^3} + 8.98 \tag{11}$$

The above detailed formulas were considered in the rest of the study for comparison with the finite element results. In addition, formulas suggested by Safar and Abou-Zeid (2014) are extended to account for the strengthening effect of CFRP strips.

3. Numerical modeling

ANSYS finite element program was used to build a three-dimensional model representing the strengthened and un-strengthened beams tested by author as listed in Safar and Abou-Zeid (2014). The experimental program included testing of twelve end-web panel steel plate girders. The selected specimens were divided into four groups according to aspect ratio, a/h, and web slenderness ratio, h/t_w. Each group consisted of three specimens: One specimen served as reference girder and the other two specimens were strengthened using CFRP strips applied at the diagonal tension direction. The number of CFRP strips were varied: One or three strips on single or both sides of the web. Fig. 1 shows the general test configuration in addition to the arrangement of CFRP strips and location of strain gauges for different specimens. All plate girders were composed of mild steel having 235 MPa yield strength, F_y, 360 MPa ultimate strength, F_u, 200 GPa Young's modulus, E, and 0.3 Poisson ratio, ν. The ratio of flange-to-web thickness, t_f/t_w, was kept constant in all specimens in order to exclude the effect of fixation of flanges-to-web plate. Double sided end stiffeners and transverse stiffeners were used at supports and loading points to exclude web crippling and local web yielding failure modes at concentrated loads. Details of dimensional properties of tested plate girders are listed in Table 2. All steel plate girders were loaded till failure. The load was applied on a spread beam by means of a hydraulic actuator with capacity of 2000 kN. In order to avoid failure

Table 2 Summary of tested beams

Test group	Designation	b_f (mm)	t_f (mm)	h (mm)	t_w (mm)	h/t_w	a (mm)	a/h	CFRP location
	CT-1-135								----
1	SC-1-135-1	165	12	540	4	135	540	1	One side
	SG-1-135-3								
	CG-1-180								----
	SG-1-180-1	165	10	540	3	180	540	1	One side
	SG-1-180-3								
	CG-2-135								----
3	SC-2-135-1	165	12	540	4	135	1080	2	One side
	SG-2-135-3								Two sides
	CG-3.5-180								----
4	SG-3.5-180-1	165	12	540	4	135	1890	3.5	One side
	SG-3.5-180-3								Two sides

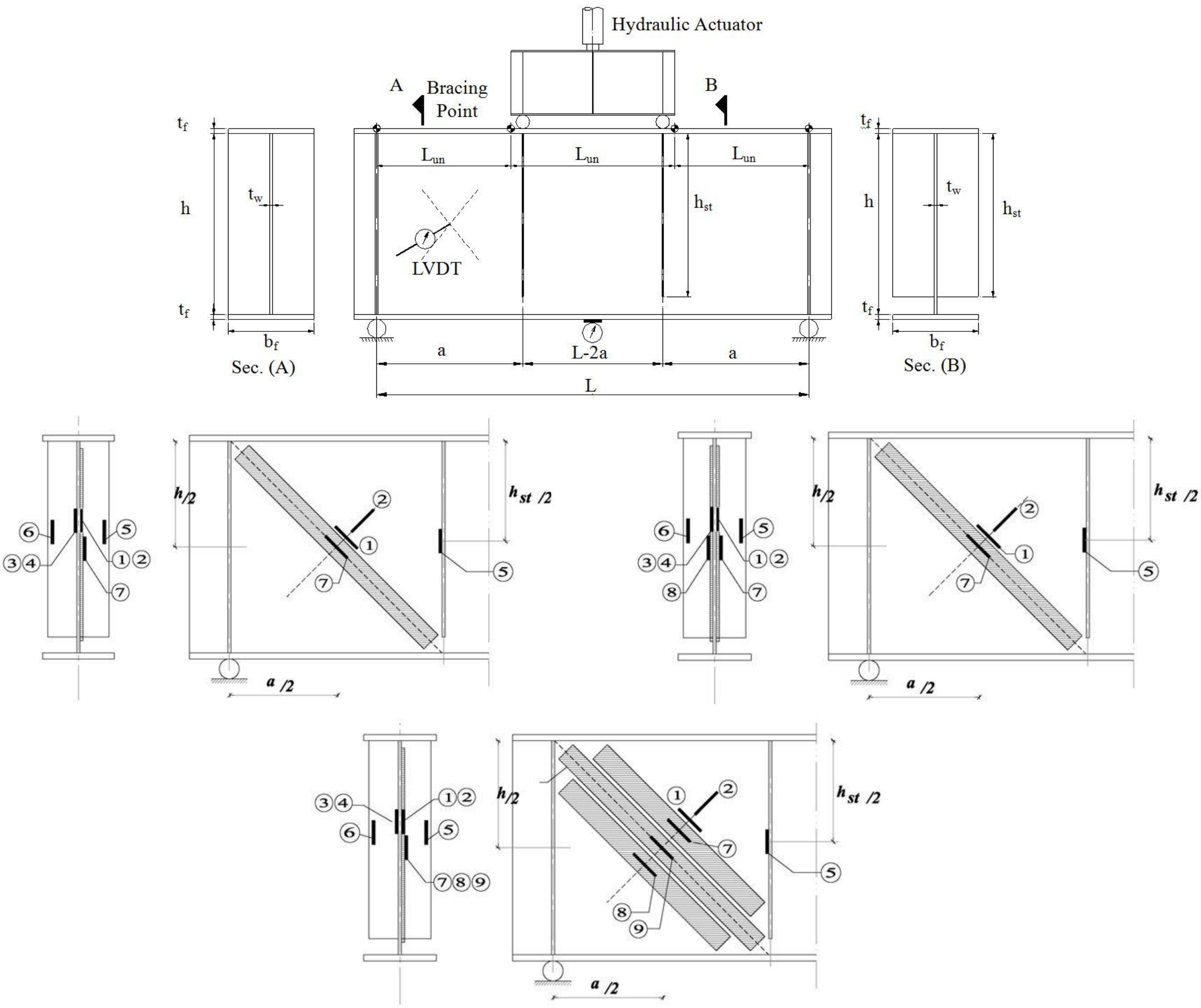

Fig. 1 General view of test set-up, Safar and Abou-Zeid (2014)

by lateral-torsion buckling, the compression flange of all specimens was braced at appropriate intervals. Vertical deflection at mid span and lateral movement at middle of end panel were tracked along test procedure by Linear Variable Deformation Transducers (LVDT), Fig. 2.

The 3-D models are built to resemble the test specimens including steel plate girder, epoxy adhesive, and CFRP strips. Solid 45 element is used to represent the different components (Peiris 2011, EL-Hacha *et al*. 2012, Roshanfekr 2012). Due to symmetry, only half of the studied beams were modeled (Fig. 3). Full bond between steel-epoxy adhesive and CFRP strips-epoxy adhesive is assumed by modeling the contact surface using common nodes. Epoxy and CFRP are positioned on one side or both sides of steel web following the experimental program. The considered thickness of CFRP and epoxy were 1.2 mm and 1.0 mm, respectively.

3.1 Materials properties

Material constitutive relation of steel is automatically computed upon defining Young's modulus, yield strength, and Poisson's ratio. The steel plate was modeled as having

Fig. 2 Test Set-up and Instrumentation, Safar and Abou-Zeid (2014)

bi-linear elastic-perfectly plastic steel material model with a yield strength of 235 MPa. Meanwhile, CFRP material is defined as a linear orthotropic stress-strain relationship with ultimate strength of 3600 MPa and Poisson's ratio of 0.22. Tensile modulus in local X-direction is defined equal to 180 GPa; whereas, in Y and Z directions, it is defined equal to 60 GPA. The epoxy material is modeled using a linear isotropic stress-strain relationship with tensile strength of 31 MPa, tensile modulus of 11200 MPa, and Poisson's ratio of 0.38. Beyond the ultimate tensile strength, a small plastic region was modeled to facilitate the identification of the failure location. The Von-Mises failure criterion, available for the material model, was used to predict the failure of the epoxy adhesive, Peiris (2011).

3.2 Loads and boundary conditions

Pressure load is applied to the top surface area of the intermediate stiffener in order to exclude web crippling and local web yielding failure modes at concentrated loads and to simulate the experimental tests. At the base of bottom flange under the same area of End-bearing stiffener, all nodes were prevented from moving in the load direction and longitudinal direction of specimen (U_x and U_y). Symmetric boundary conditions are applied at the end surface of the half model. Bracing points are simulated by preventing the lateral movement at the corresponding nodes in model as shown in Fig. 3.

3.3 Solution

The analysis conducted herein is nonlinear static analysis based on material and geometric non-linearity. Newton-Rapshon technique, imbedded in ANSYS software program, is used. Load was applied in steps with equilibrium iterations to convergence at each load step. Iterations continue till the limit load is reached based on default criteria of ANSYS program. De-bonding of CFRP strips is detected upon exceeding the plastic strain of the ultimate strain of the adhesive.

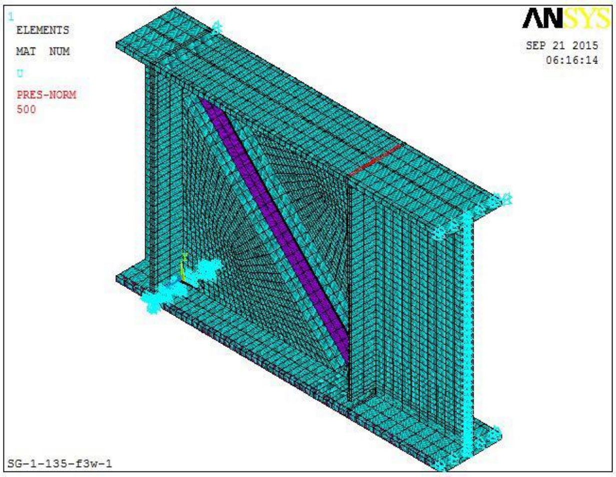

Fig. 3 FE model of half of strengthened beam

3.4 Model verification

3-D finite element models are built as detailed in previous sections. Geometric imperfections are imbedded in the models following the first Eigen mode shape while scaling values to simulate measured results during experimental tests. Accordingly, the numerical models are verified using the available experimental results. Then, the models are developed in order to expand the parametric study. In this section, the numerical and experimental results are compared to prove models validity for analysis and extension of study. In addition, the nominal and post-buckling shear strength of the simulated specimens calculated using formulas provided by well-established theories are compared to the finite element results to investigate the gain in the steel plate girder shear strength due to the proposed CFRP strengthening method.

Fig. 4 shows the stress distribution in one of specimens compared to the deformed shape of the tested specimen. As can be noted, the extent of the tension field compares to the one observed during testing. Fig. 5 shows that FE results for the nominal shear strength are compatible with the experimental test results of bare specimens; the average error is 5.5%. Meanwhile, the average error between Hoglund theory and experimental test results reaches 10%. The average error between Safar (2013) formula and experimental test results is 16.5%. However, the percentage of error reached 61% between the experimental results and Basler's theory results. This can be attributed for the fact

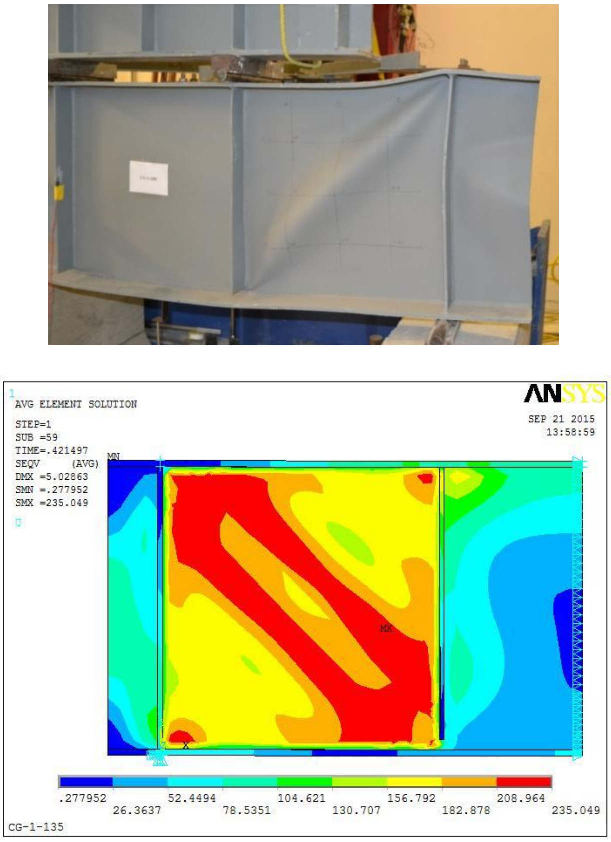

Fig. 4 Von-Mises in FEM vs. Experimental Deformed Shape for Test Unit (SG-1-135-1)

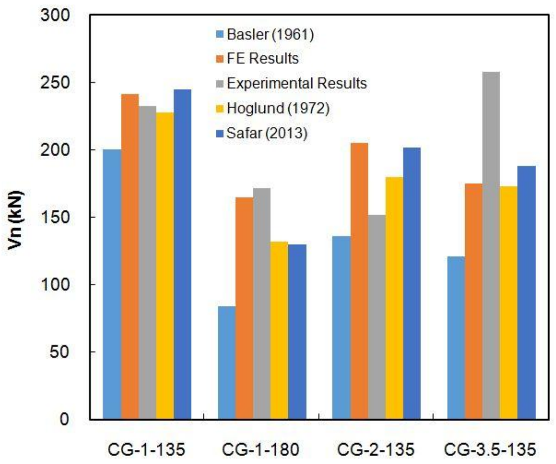

Fig. 5 FE results vs. Experimental Results and Available Formulas for Nominal Shear Strength (V_n)

that Basler theory does not account for the effect of post-buckling strength for end-web panel steel plate girder. Based on the above results, FE models are considered capable to simulate steel plate girder strengthened with CFRP strips. In addition, the preliminary analysis showed that shear strength of steel plate girder could be enhanced effectively when CFRP strips are applied at the same orientation of principal tensile stresses.

4. Parametric study

The parametric study is performed using the calibrated models to investigate the effect of different parameters which have not been covered by the experimental part of the study, Safar and Abou-Zeid (2014). The parameters included in the parametric study include: Web slenderness ratio, h/t_w; aspect ratio of steel girder, a/h; flange-to-web thickness ratio, t_f/t_w; and number of CFRP strips, n.

All the independent variables are changed within practical limits to generate ninety-six models in order to highlight the influence of each variable on non-rigid end post steel beams. Height of web plates and width of flanges in all models is assumed 1500 mm and 400 mm, respectively. These values are selected so that all steel girders will have web truss action, rather than beam action in order to enforce resistance of shear stresses through post buckling. Geometric imperfections following the first Eigen buckling mode are applied according to American Welding Society (AWS), h/67. Intermediate stiffeners with height equal to 1400 mm are proportioned as per AISC code provision (2010). The yield strength of the different models is considered equal to 235 MPa. Values of the input variables considered in the parametric study are listed in Table 3.

5. Analysis of results

The analysis of the ninety-six models representing end-web panel steel plate girder strengthened with CFRP strips on the diagonal tension direction is exhibited in this section.

Table 3 Values of parameters in parametric study

Parameter	Values
Web slenderness ratio, h/t_w	140, 180, 220, 260
Aspect ratio, a/h	0.5, 1.0, 1.5
Thickness of flange to web, t_f/ t_w	2, 6
Number of CFRP strips on both sides	2, 6, 10

Results are studied to assess the effect of the considered independent variables on ultimate shear strength of steel plate girders. The effect of each independent variable on strengthening ratio of critical shear strength (V_{crs}/V_{cru}), strengthening ratio of nominal shear strength (V_{ns}/V_{nu}), and strengthening ratio of post-buckling shear strength (V_{pbs}/V_{pbu}) is investigated. Moreover, shear strength supported by CFRP strips (V_{cfrp}) is then examined by varying the number of used strips as listed in Table 3. In the following sections, results of the performed parametric analysis are presented. The critical shear strength (V_{cr}) is based on the elastic buckling analysis results. The post buckling shear strength of bare steel specimens is calculated as the difference between nominal shear strength and elastic shear strength ($V_{pbu} = V_{nu} - V_{cr}$). Meanwhile, the post buckling shear strength of strengthened specimens is determined as the summation of the post buckling shear strength of bare steel specimens and the shear strength provided by CFRP strips ($V_{pbs} = V_{pdu} + V_{cfrp}$). The nominal shear strength of strengthened specimens is the summation of elastic shear strength and post-buckling shear strength of strengthened specimens ($V_{ns} = V_{cr} + V_{pbs}$). Meanwhile, the nominal shear strength of bare specimens is the summation of elastic shear strength and post-buckling shear strength ($V_{nu} = V_{cr} + V_{pbu}$).

5.1 Web slenderness ratio, h/t_w

AISC (2010) provisions specifies a minimum slenderness limit $(h/t_w)_{min}$ where the effect of truss action of the web panel will take place. In the current study, the different girders are proportioned such that the slenderness ratio exceeds this limit such that post-buckling stresses will be developed due to truss action resistance. However, it should be noted that, by increasing web slenderness ratio, ratio of post buckling strength to nominal strength will increase, which may affect the efficiency of using CFRP strips on the diagonal tension direction. Upon examining the results, it is found that the value of V_{cr} is not affected by the variation of slenderness ratio h/t_w from 140 to 260. In addition, the variation of the number of CFRP strips on both sides from 2 to 10 has minor effect on the shear buckling strength. Furthermore, the value of V_{cr} is not affected by the variation of t_f/t_w ratio in the range of the parametric study.

It should be noted that, in the current study, CFRP strips is not applied under direct contact with the applied forces. Therefore, the influence of using CFRP strips with intermediate modulus will not be prominent in the elastic range. Figs. 6 and 7 show the influence of increasing web slenderness ratio (h/t_w) on the ratio between post-buckling to yield shear strength. As can be seen, increasing web

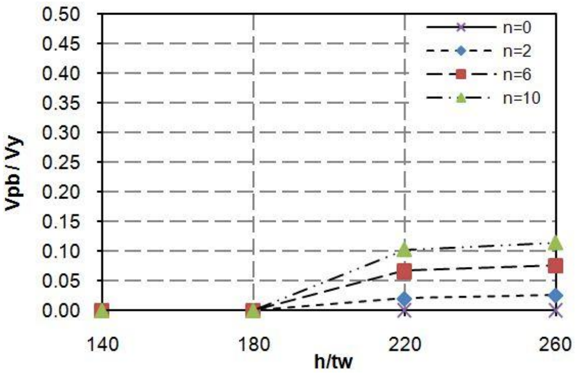

Fig. 6 Effect of h/t_w on V_{pb}/V_y for Models having a/h = 0.5 and t_f/t_w = 2.0

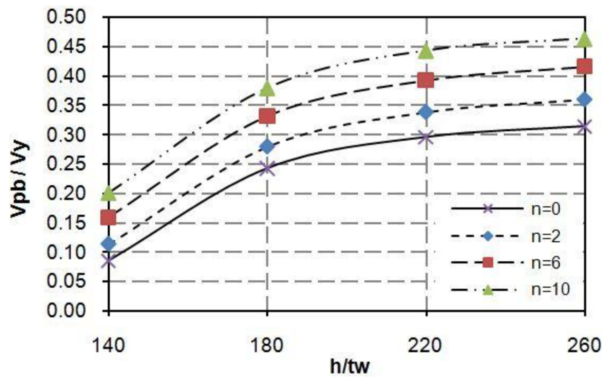

Fig. 7 Effect of h/t_w on V_{pb}/V_y for models having a/h = 1.0 and t_f/t_w = 2.0

slenderness ratio generally results in increasing the post buckling to yield shear strength. However, this influence depends on the panel aspect ratio. For aspect ratios equal to 1.0 and 1.5, this ratio increased by percentages reaching 50-80% as the slenderness ratio changes from 140 to 180. Same behavior is observed regardless of the number of added CFRP strips.

5.2 Aspect ratio of steel girder, a / h

Aspect ratio of web panel had a great effect on ultimate shear strength and buckling mode shape. Different design codes implement aspect ratio as a main factor in calculating buckling coefficient factor (K). The performed parametric study indicated that the variation of a/h affects the inclination angle of tension field action in addition to buckling mode shape. Maximum enhancement of using CFRP strips is observed for units having aspect ratio equal to 1.0. Figs. 8(a), (b), (c) and (d) show the influence of variation of aspect ratio on the post buckling to yield strength for selected units. As can be seen, for aspect ratio equal to 0.5 and slenderness ratios less than 180, the post-buckling shear strength is almost zero since the shear capacity is governed by yielding. This coincides with the

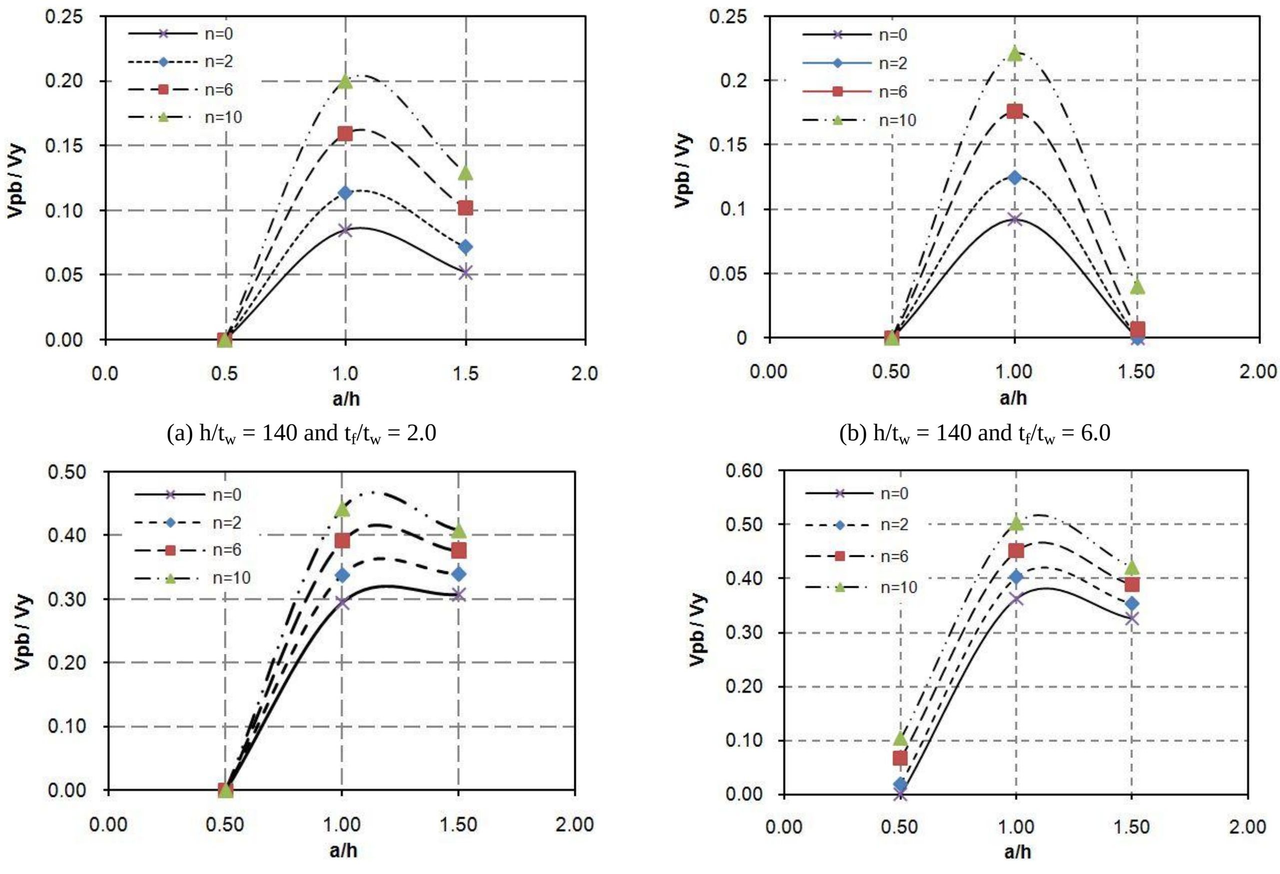

(a) h/t_w = 140 and t_f/t_w = 2.0

(b) h/t_w = 140 and t_f/t_w = 6.0

(c) h/t_w = 220 and t_f/t_w = 2.0

(d) h/t_w = 220 and t_f/t_w = 6.0

Fig. 8 Effect of a/h on V_{pb}/V_y

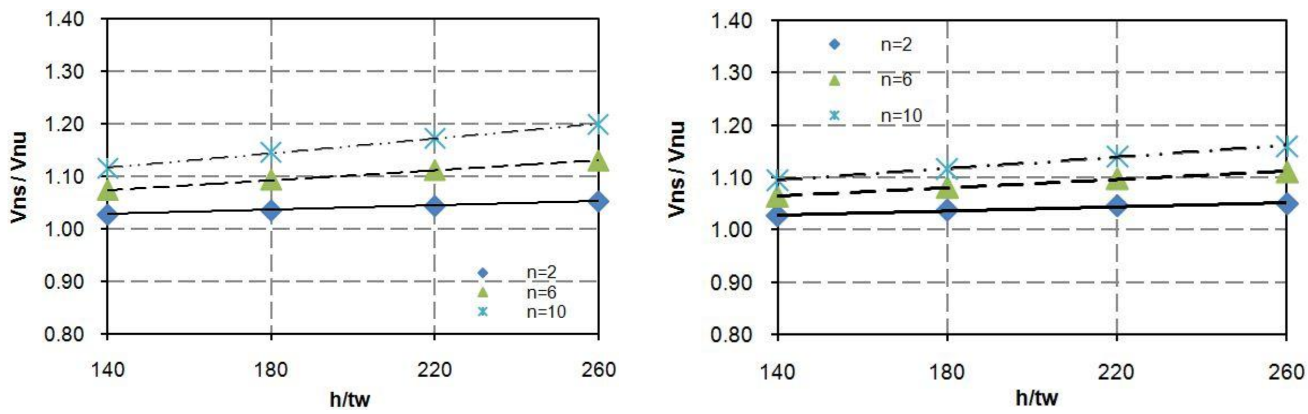

(a) $t_f/t_w = 2.0$ (b) $t_f/t_w = 6.0$

Fig. 9 Effect of h/t_w on V_{ns}/V_{nu} for a/h = 0.5

assumptions made by AISC code (2010), Hoglund theory (1972), and mathematical model proposed by Safar (2013). On the other hand, for aspect ratio equal to 0.5 and slenderness ratio greater than 180, post-buckling strength is developed for models having flange-to-web thickness equal to 6.0. It is also noted that for aspect ratio equal to or higher than 1.0 and web slenderness ratio equal to or larger than 180, post-buckling strength for un-strengthened specimens is almost constant with an average value of $0.3V_y$. Meanwhile, increase in the post buckling strength is observed for models having aspect ratio equal to 1.0 and 1.5.

The maximum increase in post-buckling strength is found equal to $0.5V_y$ for models having aspect ratio equal to 1.0, web slenderness ratio equal to 220, and flange-to-web thickness equal to 6.0. This is attributed to the fact that, at aspect ratio 1.0, tension field action is diagonally oriented in the same direction of the applied CFRP strips. In addition, as the flange-to-web thickness increases, the boundary condition at the web to flange junction is enhanced leading to increasing the post buckling strength. And finally, increasing the web slenderness ratio leads to full utilization of the elastic buckling zone.

5.3 Flange-to-web thickness, t_f/t_w

The web panel elastic buckling load is pronounced by increasing the flange-to-web plate thickness. This is attributed to the fact that increasing t_f/t_w ratio provides a considerable rotational restraint to the web plate at flange-web juncture. However, the post-buckling strength is not considerably affected by increasing t_f/t_w ratio. Hoglund (1972) was the first researcher to include the effect of flange-to-web thickness on the nominal shear strength in term of load carrying approach by formation of plastic hinges. The mathematical model proposed by Safar (2013) assumed that flanges change the boundary condition of the web at the junction between flanges to web. Accordingly, the buckling coefficient (K) will be based on boundary conditions that are more rigid than simple boundary conditions and less rigid than fixed boundary conditions.

In the current study, flange-to-web ratio (t_f/t_w) ratio is varied from 2.0 to 6.0 in order to study the effect of adding CFRP strips while considering different boundary conditions of the web. By examining Fig. 8, influence of changing t_f/t_w ratio can be noticed on post buckling shear resistance values. By variation of t_f/t_w ratio from 2 to 6, the post buckling strength (V_{pb}) increased by a percentage equal to 5%. Such increase is expected to affect the nominal shear strength. Analysis of results revealed that the variation of strengthening ratio of nominal shear strength (V_{ns}/V_{nu}) is mainly controlled by web slenderness ratio (h/t_w). The percentage of enhancement of strengthening ratio (V_{ns}/V_{nu}) is 5% on average for n equal to 2.0 and t_f/t_w equal to 2.0 as web slenderness ratio (h/t_w) increases from 140 to 260. Whereas, strengthening ratio is enhanced by 2.5% on average for n equal to 2.0 and t_f/t_w equal to 6.0 as web slenderness ratio (h/t_w) increases from 140 to 260. Also, the enhancement of strengthening ratio V_{ns}/V_{nu} is 8% on average for n equal to 6.0 and t_f/t_w equal to 2.0 as web slenderness ratio (h/t_w) increases from 140 to 260. Meanwhile, strengthening ratio is enhanced by 4% on average for n equal to 6.0 and t_f/t_w equal to 6.0 as web slenderness ratio (h/t_w) increases from 140 to 260. Additionally, the enhancement of strengthening ratio V_{ns}/V_{nu} is 12% on average for n equal to 10 and t_f/t_w equal to 2.0 as web slenderness ratio (h/t_w) increases from 140 to 260. Whereas, strengthening ratio was enhanced by 6% on average for n equals to 10 and t_f/t_w equals to 6.0 with the same increment of h/t_w.

Fig. 10 shows that the increment of nominal shear strength of strengthened specimens, having CFRP strips applied on both sides of diagonal tension direction, is directly proportional to web slenderness ratio (h/t_w) and number of CFRP strips (n). Meanwhile, the increment in nominal shear strength is directly proportional to aspect ratio (a/h) in the range of 0.5 to 1.0 and inversely proportional to a/h in the range of 1.0 to 1.5. Such increase is significantly noticed at higher values of h/t_w and n, whereas for lower values of t_f/t_w.

It is obvious from results that strengthening ratio is directly proportional to web slenderness ratio and number of CFRP strips on both sides. This is attributed to the fact that increasing web slenderness ratio (h/t_w) transfers shear resistance zone from yielding to inelastic buckling. Therefore, the nominal shear resistance for un-strengthened

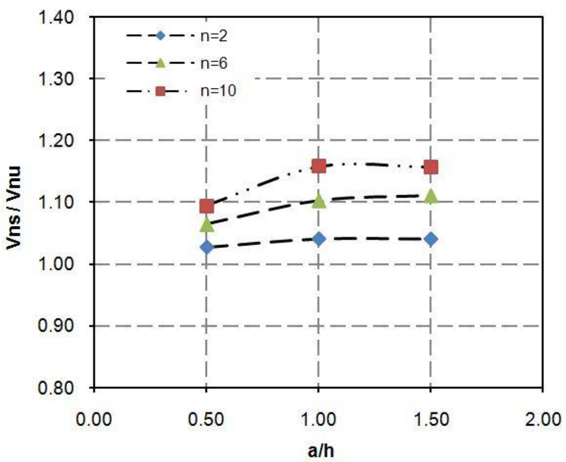

Fig. 10 Effect of a/h on V_{ns}/V_{nu} for h/t_w = 140 and t_f/t_w = 6.0

specimens, V_{nu}, has significantly decreased. As a result, the strengthening ratio will be more pronounced.

It is also observed that the maximum strengthening ratio V_{ns}/V_{nu} exists at aspect ratio 1.0. Thereby, at aspect ratio 1.5, strengthening ratio decreases by 5% compared to values noted at aspect ratio 1.0. Also, at aspect ratio 0.5, the minimum strengthening ratio is observed with percentage of decrease equal to 10% compared to values noted at aspect ratio 1.0. This is attributed to the fact that tension field action has an angle of 45 ^{o} with the vertical. As a result, tension field action will have the same inclination angle of diagonal tension direction where CFRP strips are applied at aspect ratio equals 1.0.

5.4 Number of CFRP Strips, *n*

The number of CFRP strips is varied from 2 to 6 and considering applying strips on single side or both sides of web. The geometric dimension of each CFRP strip is 50×1.2 mm. Accordingly, the effect of web slenderness ratio (h/t_w), end-web panel aspect ratio (a/h), number of CFRP strips on both sides (n), and flange-to-web thickness ratio, (t_f/t_w) on CFRP strips shear strength and CFRP strips efficiency ratio is investigated. CFRP strips are orthotropic materials where maximum load transfer exists at the direction of CFRP fibers. The value of shear strength offered by CFRP strips equals the difference between nominal shear strength of strengthened specimens and nominal shear strength shear of un-strengthened specimens ($V_{CFRP} = V_{ns} - V_{nu}$). In addition, the value of CFRP strips shear strength can be expressed as difference between post-buckling shear strength of strengthened specimens and post-buckling shear strength of un-strengthened specimens ($V_{CFRP} = V_{pbs} - V_{Pbu}$). In the current study, no effect is observed on the elastic buckling strength from the applied strengthening procedure.

Generally, by applying CFRP strips on the diagonal tension direction of end-web panel of steel plate girder, epoxy adhesive is pronounced as the main reason of de-bonding failure when the maximum stresses of epoxy are reached. Therefore, the efficiency of CFRP strips depends on epoxy adhesive mechanical properties. Maximum tension force (T_{bond}) supported by CFRP strips before de-bonding failure takes place in epoxy adhesive can be expressed as follow

$$T_{\text{bond}} = E_{\text{CFRP}} \times \varepsilon_{\text{epoxy}} \times t_{\text{CFRP}} \times b_{\text{CFRP}} \times n \qquad (12)$$

Where: E_{CFRP} is the modulus of elasticity of CFRP strips in principle direction of CFRP strips; ε_{epoxy} is the maximum tensile strain of epoxy adhesive; t_{CFRP} and b_{CFRP} are the thickness and width of CFRP strip, respectively; and n is the number of applied CFRP strips.

Figures shown in previous sections indicate that the percentage of enhancement in post-buckling strength due to the applied CFRP strips on both sides of web is 4%V_y, 8%V_y, and 12%V_y on average for n equal to 2, 6, and 10, respectively.

The strengthening ratio is examined for the different studied models**.** Minimum increment in strengthening ratio (V_{ns}/V_{nu}) of end-web panel steel plate girder is for beam having h/t_w of 140 and a/h of 0.5. For this beam, the value of V_{ns}/V_{nu} increased from 1.025 to 1.10 as the number of CFRP strips increased from 2 to 10 for t_f/t_w equal to 6.0. Whereas, for beam having t_f/t_w equal to 2.0, the value of V_{ns}/V_{nu} increased from 1.03 to 1.12 for the same increase of number of CFRP strips. It is noted that the influence of t_f/t_w on strengthening ratio V_{ns}/V_{nu} is inconsiderable for n equal to 2 and had a little increment by 2% for n equal to 10. On the other hand, the maximum increment in strengthening ratio V_{ns}/V_{nu} of end-web panel steel plate girder is observed for beam with h/t_w equal to 260 and a/h equal to 1.0. For this beam, the value of V_{ns}/V_{nu} increased from 1.10 to 1.30 with the increase of n from 2 to 10 for t_f/t_w equal to 2.0. Whereas, for beam with t_f/t_w equal to 6.0, the value of V_{ns}/V_{nu} increased from 1.07 to 1.25 with the increase of n from 2 to 10. In addition, number of CFRP strips on both sides has no observed effect at n equal to 2.0 for different values of a/h. However, for higher values of n, the maximum strengthening ratio is clearly noticed at aspect ratio equal to 1.0.

Figs. 11 and 12 show the variation of shear strength supported by CFRP strips (V_{CFRP}) with respect to end-web panel aspect ratio (a/h), web slenderness ratio (h/t_w) while considering different values of flange-to-web thickness (t_f/t_w) for each number of CFRP strips (n) considered in the parametric analysis. Shear strength supported by CFRP strips is normalized to present results in a non-dimensional form as a CFRP strips efficiency ratio. It can be noted

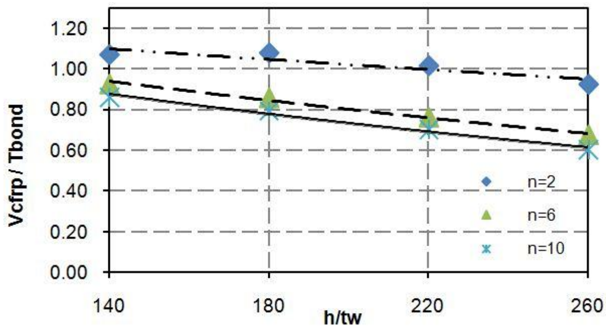

Fig. 11 Effect of h/t_w on V_{CFRP}/T_{bond} for a/h = 1.0 and t_f/t_w = 2.0

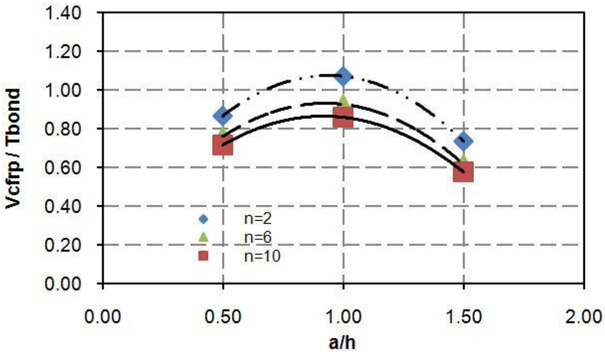

Fig. 12 Effect of a/h on V_{CFRP}/T_{bond} for h/t_w = 140 and t_f/t = 2.0

that the efficiency of CFRP strips increased by applying CFRP strips on both sides of diagonal tension direction. Meanwhile, it is inversely proportional to web slenderness ratio (h/t_w). Whereas, the efficiency of the applied CFRP strips is directly proportional to a/h from 0.5 to1.0 and inversely proportional to a/h from 1.0 to 1.5. Such increase is magnified at lower values of h/t_w and higher values of n. However, the effect of t_f/t_w is not noticed. Analysis of parametric study results revealed that the variation of efficiency ratio is mainly controlled by web slenderness ratio h/t_w. Efficiency ratio decreased by 15% on average for n equal to 2.0 and t_f/t_w equal to 2.0 as the web slenderness ratio increased from 140 to 260. Whereas, efficiency ratio reduces by 30% on average for n equals to 2.0 and t_f/t_w

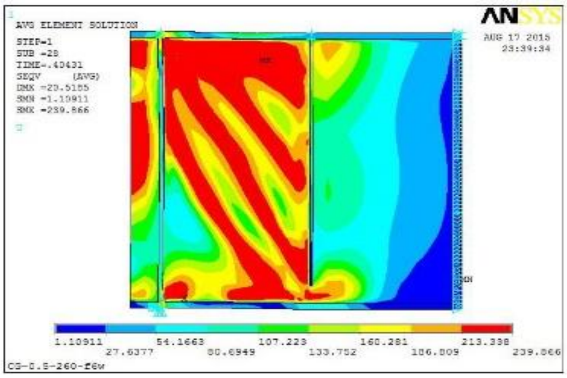

Strengthened model

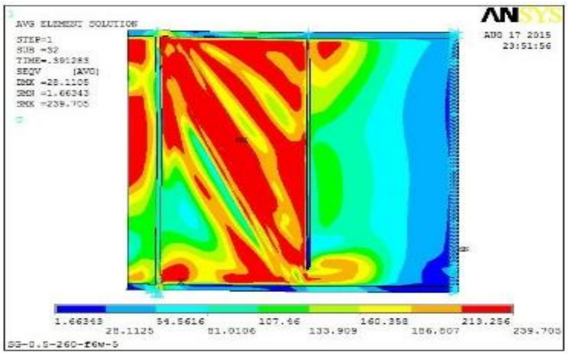

Bare steel model

(a) Aspect ratio a/h = 0.5

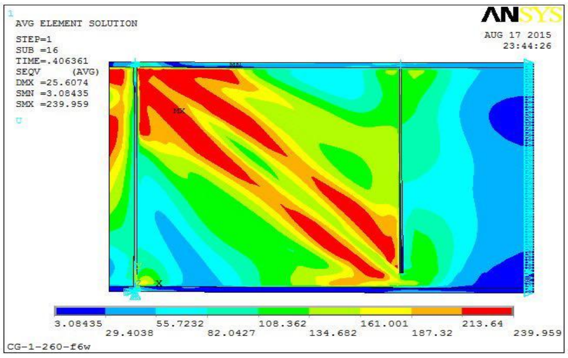

Strengthened model

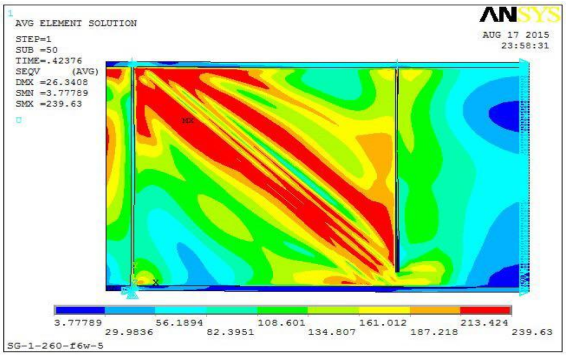

Bare steel model

(b) Aspect ratio a/h = 1.0

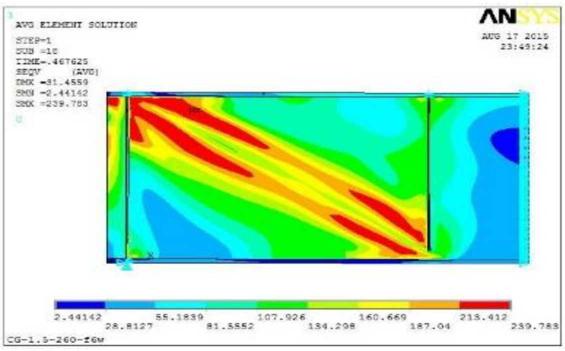

Strengthened model

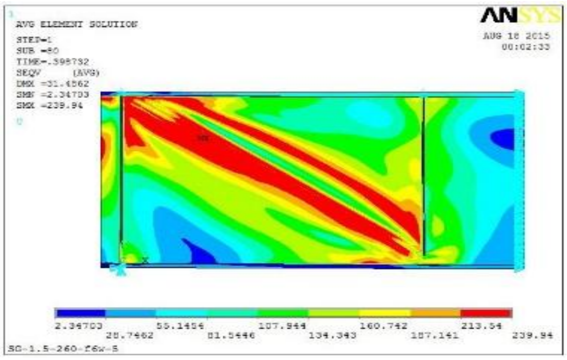

Bare steel model

(c) Aspect ratio a/h = 1.5

Fig. 13 Effect of CFRP strips on distribution of Von Mises Stresses

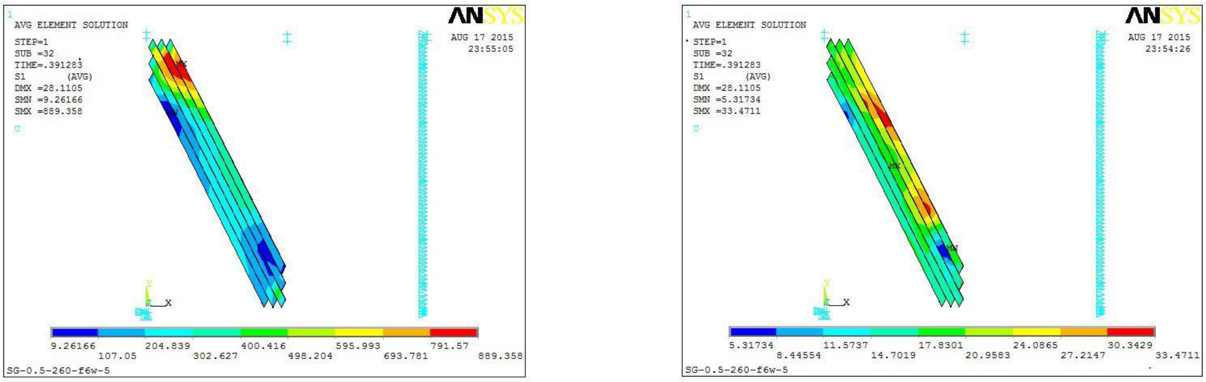

(a) Aspect ratio a/h = 0.5

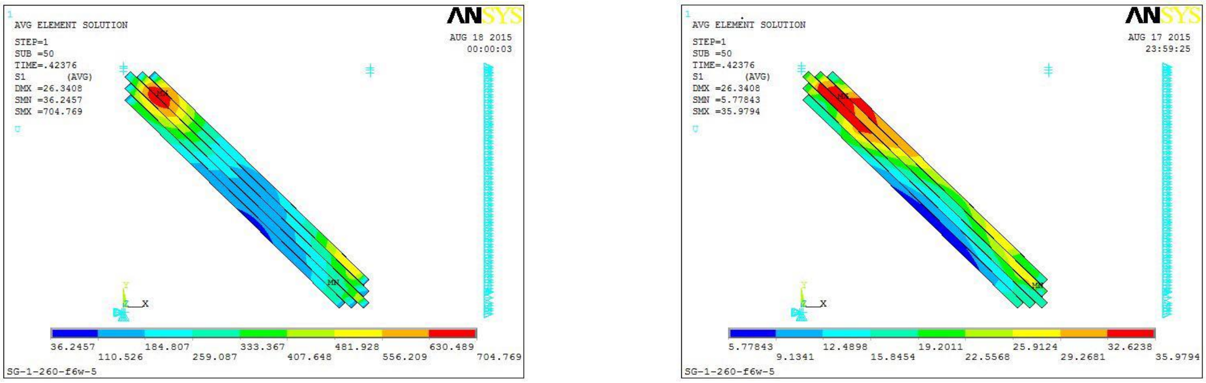

(b) Aspect ratio a/h = 1.0

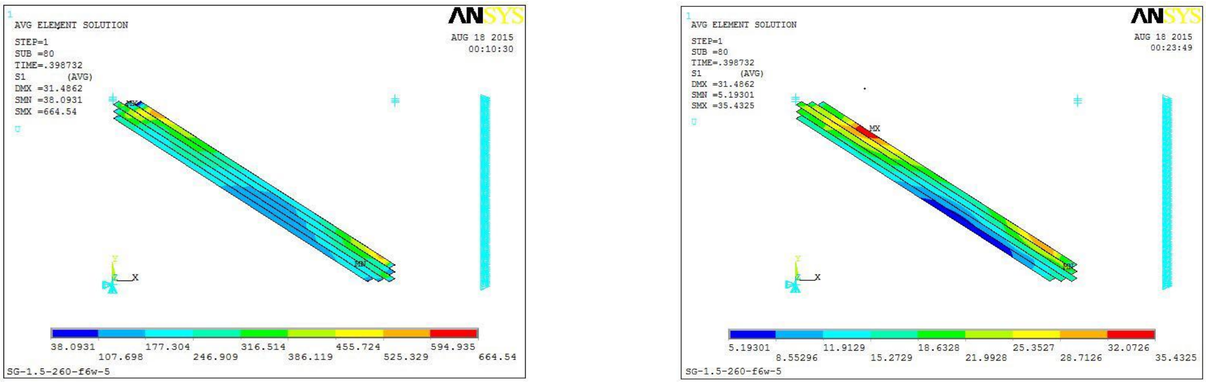

(c) Aspect ratio a/h = 1.5

Fig. 14 Maximum Principal Stresses for CFRP strips and Epoxy Adhesive

equal to 6.0 with the same increment of h/t_w. Also, efficiency ratio decreases by 12% on average for n equal to 6.0 and t_f/t_w equal to 2.0 with the same increment of h/t_w. Whereas, efficiency ratio reduces by 30% on average for n equal to 6.0 and t_f/t_w equal to 6.0 with the same increment of h/tw. Additionally, efficiency ratio decreases by 12% on average for n equal to 10 and t_f/t_w equal to 2.0 with the same increment of h/t_w. Whereas, efficiency ratio reduces by 30% on average for n equals to 10 and t_f/t_w equals to 6.0 with the same increment of h/t_w.

It is obvious from results that the strengthening ratio is inversely proportional to web slenderness ratio and number of CFRP strips on both sides. This is attributed to the fact that increasing of web slenderness ratio h/t_w transfers shear resistance zone from yielding to inelastic buckling at higher values of h/t_w. Therefore, yielding zone is decreased leading to decreasing the width of diagonal tension field action. Thereby, the probability of utilization of all the applied CFRP strips on the diagonal tension direction is reduced. In the same manner, efficiency ratio is also inversely proportional to CFRP strips number.

5.5 Mode of failure

For the bare steel and strengthened models, failure modes and distribution of stresses are examined. Figs. 13 and 14 show the variation of diagonal tension stresses for bare and strengthened specimens and the corresponding mode of failure. It is found that CFRP strips have a significant effect on stress distribution at end-web panel.

This can be observed through the concentration of stresses along diagonal tension direction. It is also noted that the maximum principle stresses observed in CFRP strips are inversely proportional to a/h. As the aspect ratio of the girder changed from 0.5 to 1.0 and 1.5; the maximum principle stresses decreased by percentages reaching 20.8% and 25.3%, respectively. For the different models, the observed failure mode is de-bonding of CFRP strips when the epoxy adhesive reached its maximum shear strength.

6. Mathematical modeling of shear strength of strengthened end-web panels

Shear strength of End-web panels strengthened with CFRP strips applied on the diagonal tension direction is governed by de-bonding of CFRP strips (failure of epoxy adhesive) as illustrated in previous sections. CFRP strips applied in the diagonal tension direction can effectively enhance nominal shear strength and magnify the effectiveness of tension field action on steel yielding. Nominal shear strength of end-web panels strengthened with CFRP strips exceeds the nominal shear strength of bare end-web panels by percentages reaching about 22-30%. In this section, a formula predicting the shear strength of strengthened end-web panels is formulated based on the parametric analysis results.

As discussed in Section 2, numerous formulas are available to express the nominal shear strength of bare end-web panels of steel girders. In the current study, Hoglund theory is applied to the mathematical model to expresses the nominal shear strength of end-web panels strengthened with CFRP strips on diagonal tension direction as it provides the most accurate results when compared to the available experimental or numerical results, Safar (2013).

$$V_{ns} = \left(V_w + V_f\right)_{\text{Hoglund}} + V_{\text{CFRP}} \tag{13}$$

Where V_w is the shear strength supported by web according to Hoglund theory, V_f is the shear strength supported by flange according to Hoglund theory, and V_{CFRP} is the shear strength supported by CFRP strips.

Based on analysis of the parametric study results, shear strength supported by CFRP strips, V_{CFRP}, is found mainly dependent on the mechanical properties of epoxy adhesive. Thereby, it will affect the formula estimating V_{CFRP}. In addition, web slenderness ratio and aspect ratio have a great effect on V_{CFRP}, whereas, flange-to-web thickness ratio does not show a steady reliable effect. As a result, V_{CFRP} is estimated as follows

$$V_{\text{CFRP}} = \Phi \times T_{\text{bond}} \tag{14}$$

$$T_{\text{bond}} = E_{\text{CFRP}} \times \varepsilon_{\text{epoxy}} \times A_{\text{CFRP}} \times n \tag{15}$$

$$A_{\text{CFRP}} = b_{\text{CFRP}} \times t_{\text{CFRP}} \tag{16}$$

Where Φ is efficiency ratio, T_{bond} is maximum tension force supported by CFRP strips before de-bonding failure takes place, E_{CFRP} is the modulus of elasticity of CFRP strips, ε_{epoxy} is the maximum tensile strain supported by epoxy adhesive, A_{CFRP} is cross sectional area of one CFRP strip, and n is the number of CFRP strips on both sides.

As shown in Eq. (15), T_{bond} is significantly depending on maximum tensile strain of epoxy adhesive, instead of, depending on maximum strain of CFRP strips, because failure is occurred at the epoxy adhesive as a de-bonding failure. The efficiency ratio (Φ) is included to account for the independent variables effecting on the shear strength supported by CFRP strips based on regression analysis of the parametric study results as follows

$$\Phi = \zeta \times \alpha \times \beta \tag{17}$$

$$\zeta = 0.6 \times \left\{1 - 0.003\left(\frac{h}{t_w}\right) - 140\right\} \leq 1.0 \tag{18}$$

$$\alpha = \frac{\sqrt{a^2 + h^2}}{\text{Bigger of (a or h)}} \tag{19}$$

$$\beta = 0.75 \times \frac{h}{1500} - 0.25 \tag{20}$$

Where ζ is web slenderness reduction factor, α is aspect ratio magnification factor, and β is height of web factor.

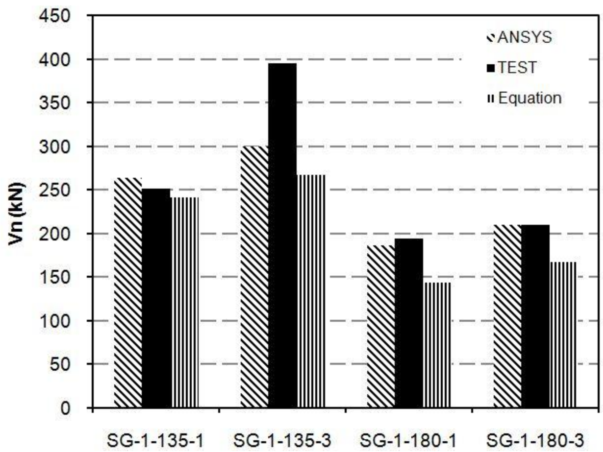

Fig. 15 Proposed formula results compared to tests and FE results

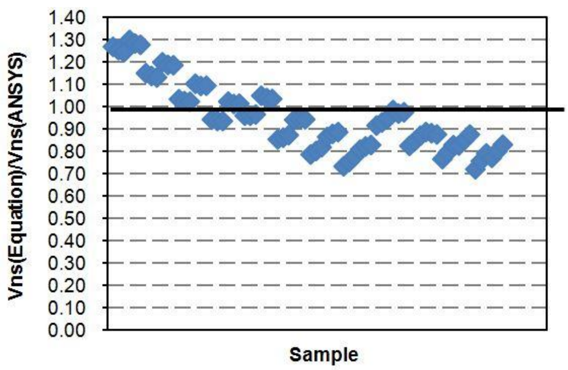

Fig. 16 Proposed formula results compared to and FE results

Fig. 15 show a comparison between shear strength results from experimental tests, finite element models, and proposed formula. As can be seen, the difference between estimates provided by formula and FE results range between 8% and 23%. Meanwhile, the difference between estimates provided by formula and test results range between 4% and 32%.

Fig. 16 shows the difference between nominal shear strength for strengthened models calculated by finite element models and by proposed equation with variation of all strengthened parametric study models. The average value was 0.95, minimum value was 0.72, maximum value was 1.30 and standard deviation was 0.15.

7. Conclusions

In this research, the ultimate strength of end-web panel of steel plate girder strengthened with CFRP strips was investigated. Theoretical shear strength equations of end-web panels were presented with an explanation of stages of failure of steel plate girder due to pure shear. An outline of previous experimental and numerical research work on steel plate girders strengthened with CFRP strips was presented considering shear strengthening. Afterwards, a finite element model was established to represent end-web panel of steel plate girder strengthened with CFRP strips under pure shear using the general purpose finite element program ANSYS. The numerical solution results were compared to test results conducted by one of the authors. It was shown that the numerical model provided reliable results compared to test since the maximum difference between test and finite element model solution did not exceed 8%. After verifying the numerical solution, a comprehensive parametric analysis was conducted to investigate the effect of CFRP strips on nominal shear strength. The main conclusions drawn from the performed parametric study include the following:

- Shear strengthening of end-web panel steel plate girder by CFRP strips on the diagonal tension direction has no effect on the elastic shear strength due to the low value of modulus of elasticity of applied CFRP strips compared to modulus of elasticity of steel plate girder.
- It is noted that, the effect of web slenderness ratio on strengthening ratio V_{ns}/V_{nu} was significant when h/t_w equals 140, 180 for aspect ratios of 1.5 and flange-to-web thickness of 6.0. This was attributed for the enhancement in boundary conditions at the flange to web conjunction and the coincidence of the inclination of tension field action with the diagonal direction where CFRP strips were applied.
- The enhancement in post buckling strength due to the applied CFRP strips on both sides was found equal to by 4%, 8% and 12% of yield shear strength on average for n equal to 2, 6, and 10, respectively. Also, by the variation of t_f/t_w from 2 to 6, the post buckling shear strength (V_{pb}) had an increment of 5% of the yield shear strength. In addition, the maximum post-buckling strength was obtained at aspect ratio of 1.0.
- The enhancement in nominal shear strength due to bonding CFRP strips is directly proportional to web slenderness ratio (h/t_w) and number of used CFRP strips (n). Meanwhile, the maximum enhancement in nominal shear strength is observed at aspect ratio (a/h) = 1.0. At this ratio, the orientation of CFRP strips coincides with the direction of principal tensile stresses in the web after buckling. This enhancement is magnified at higher values of h/t_w and n. However, flange-to-web thickness (t_f/t_w) has minor effect on increment in post buckling strength.
- The variation of h/t_w from 140 to 260 showed that the strengthening ratio increased by 12.5% on average, whereas, the portion of load supported by CFRP strips (V_{CFRP}) decreased by 30%.
- The variation of a/h from 0.5 to 1.0 showed that the strengthening ratio increased by 10% and load supported by CFRP strips (V_{CFRP}) increased by 20%. Whereas, the variation of a/h from 1.0 to 1.5 showed that the strengthening ratio resulted in decreasing strengthening ratio by 5% and load supported by CFRP strips (V_{CFRP}) by 14%.
- Mode of failure for all specimens included in the verification and parametric study results in the finite element model was observed to be deboning of CFRP strips.

Numerical results of the parametric analysis were used to develop formulas that can be used to estimate the nominal shear strength of strengthened end-web panels of plate girders in the range of the independent variables included in parametric analysis.

References

AISC (2010), American Institute of Steel Construction specification for structural steel buildings, Load and Resistance Factor Design, Chicago, IL, USA.

Ardalani, G.T., Showkati, H., Teymourlouei, H.E. and Firouzsalari, S.E. (2017), "The performance of plate girders reinforced with CFRP plates of various lengths", *Thin-Wall. Struct.*, **120**, 105-115.

Basler, K. (1961), "Strength of plate girders in shear", Leheigh University, Institute of Research, Report No. 251-201.

Bocciarelli, M., Colombi, P., D'Antino, T. and Fava, G. (2018), "Intermediate crack induced de-bonding in steel beams reinforced with CFRP plates under fatigue loading", *J Eng. Struct.*

EL-Hacha, R., Zangeneh, P. and Omran, H.Y. (2012), "Finite element modeling of steel-concrete composite beams strengthened with prestressed CFRP plate", *Int. J. Struct. Stab. Dyn.*, **12**(1), 23-51.

Elchalakani, M. and Fernando, D. (2012), "Plastic mechanism analysis of unstiffened steel I-section beams strengthened with CFRP under 3-point bending", *Thin-Wall. Struct.*, **53**, 58-71.

Hoglund, T. (1972), "Design of thin plate I-girders in shear and bending with special reference to web buckling", Division of Building Statics and Structural Engineering, Royal Institute of Technology, Stockholm.

May, I.M. and Bhutto, M.H. (2013), "Use of FRP composites for strengthening of slender steel web panels subjected to shear", *Proceedings of the Advanced Composites in Construction*

(ACIC), 152-164.

Miller, T.C., Chajes, M.J., Mertz, D.R. and Hastings, J.N (2001), "Strengthening of a steel bridge girder using CFRP plates", *J. Bridge Eng.*, **6**(6), 514-522.

Narmashiri, K., Jumatt, M.Z. and Sulong, N.H. (2010), "Shear Strengthening of Steel I-beams by using CFRP strips", *Sci. Res. Essays*, **5**(16), 2155-2168.

Okuyama, Y., Miyashita, T. and Wakabayashi, D. (2012), "Shear buckling test for steel girder bonded CFRP on its web", Ph.D. Disseration; Nagaoka University of Technology, Japan.

Park, J.W. and Yoo, J.H. (2015), "Flexural and compression behavior for steel structures strengthened with carbon fiber reinforced polymers (CFRPs) strip", *Steel Compos. Struct., Int. J.*, **19**(2), 441-465.

Peiris, N.A. (2011), "Steel beams strengthened with ultra-high modulus CFRP laminates", Ph.D. Dissertation; University of Kentucky, Lexington, KY, USA.

Rizkalla, S., Kazem, H. and Kobayashi, A. (2017), "Small-diameter CFRP strands for shear strengthening of steel bridge girders", *Proceedings of The 13th International Workshop on Advanced Smart Materials and Smart Structures Technology*, Japan.

Roshanfekr, H.B. (2012), "FRP stiffener efficiency coefficient for SBS shear strengthening applications", M.Sc. Disseration; Louisiana State University, Baton Rouge, LA, USA.

Safar, S.S. (2013), "Shear strength of end-web panels", *Thin-Wall. Struct.*, **67**, 101-109.

Safar, S.S. and Abou-Zeid, M.N. (2014), "Experimental investigation on shear strength of elastic of elastic end-web panels strengthened with CFRP strips", *Proceedings of Structural Stability Research Council*, Toronto, Canada.

Swanson Analysis Systems (1970), ANSYS Release 14.0, Houston, LA, USA.

Timoshenko, S.P. and Gere, J.M. (1961), *Theory of Elastic Stability*, (2nd Ed.), McGraw-Hill Book Co., Inc., New York, NY, USA.

Wagner, H. (1931), "Flat strip metal girder with very thin metal web", National Advisory Committee for Aeronautics.

Wang, L., Hou, W., Han, H. and Huo, J. (2015), "Repair of flange damage steel-concrete composite girders using CFRP sheets", *Struct. Eng. Mech., Int. J.*, **55**(3), 511-523.

CC